ACS APPLIED MATERIALS & INTERFACES

Research Article

www.acsami.org

MOF–Bacteriophage Biosensor for Highly Sensitive and Specific Detection of *Staphylococcus aureus*

Neha Bhardwaj,[†,‡] Sanjeev K. Bhardwaj,[†,‡] Jyotsana Mehta,[†,‡] Ki-Hyun Kim,*[,§] and Akash Deep*[,†,‡]

[†]CSIR-Central Scientific Instrument Organisation (CSIR-CSIO), Chandigarh 160030, India

[‡]Academy of Scientific and Innovative Research (AcSIR-CSIO), Chandigarh 160030, India

[§]Department of Civil and Environmental Engineering, Hanyang University, 222 Wangsimni-Ro, Seoul 04763, Korea

Supporting Information

ABSTRACT: To produce a sensitive and specific biosensor for *Staphylococcus aureus,* bacteriophages have been interfaced with a water-dispersible and environmentally stable metal–organic framework (MOF), NH_2-MIL-53(Fe). The conjugation of the MOF with bacteriophages has been achieved through the use of glutaraldehyde as cross-linker. Highly sensitive detection of *S. aureus* in both synthetic and real samples was realized by the proposed MOF–bacteriophage biosensor based on the photoluminescence quenching phenomena: limit of detection (31 CFU/mL) and range of detection (40 to 4×10^8 CFU/mL). This is the first report exploiting the use of an MOF–bacteriophage complex for the biosensing of *S. aureus*. The results of our study highlight that the proposed biosensor is more sensitive than most of the previous methods while exhibiting some advanced features like specificity, regenerability, extended range of linear detection, and stability for long-term storage (even at room temperature).

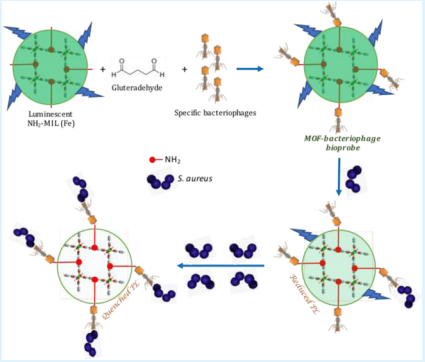

KEYWORDS: *Staphylococcus aureus, bacteriophages, MOF, fluorescence, detection*

1. INTRODUCTION

Bacterial contamination in foods (like raw meat, milk, seeds, vegetables, and water) is a cause of many health related problems.[1−4] Bacteria can transfer through cross-contamination during food preparation, ultimately reaching the food supply chain. In most nations, pathogenic contamination of food is regulated below a particular safety limit to secure the general public health. The authorities throughout the world are toughening the standards of food safety. For instance, *Staphylococcus aureus* does not produce entertoxins until about $>10^4$ CFU/g. Nonetheless, the numbers of this pathogen and other coagulase-positive staphylococci should be maintained at a much reduced level, possibly <100 CFU/g or even lower.[5,6] Food products for infants and medical patients are suggested to conform to even stricter standards.

With regard to the quantitative/qualitative analysis of bacteria, culture-based methods are the most commonly used ones. This technique nonetheless involves time-consuming steps such as sample pre-enrichment, selective enrichment, and bacterial colony isolation on selective agar plates. At times, these laborious practices may also undesirably lead to false results in the absence of typical colonies. Bacterial detection is also performed with other methods (e.g., immunological assays (ELISA, agglutination test, etc.) and nucleic acid amplification (polymerase chain reaction (PCR), colony-PCR, RT-PCR, etc.)).[7−11]

Biosensors for the detection of bacteria allow a rapid and convenient option. Several optical and electrochemical bio- and nanobiosensors have been proposed in the literature.[12−17] In particular, the optical biosensors are considered more advantageous in terms of user-friendliness, high sensitivity, and applicability toward a variety of sample types (solid, liquid, or gas). The sensitive optical biosensors for bacteria may be classified on the basis of the involved nanomaterials, including dye-doped silica nanoparticles, quantum dots, carbon dots, and fluorescent polymers.[18−21] For these optical biosensors, a list of recognition molecules (e.g., antibodies, nucleic acids, enzymes, and whole cells) are in most cases employed to detect the target analyte(s) of interest.[22−29]

Over the past decade, metal–organic frameworks (MOFs) have emerged as important multifunctional materials. They have been explored for various technological applications including gas storage, gas separation, catalysis, optoelectronics, immobilization, and sensing.[30−38] The basic structure of the MOFs consists of metal ions linked to organic ligands through coordinate bonds. A judicious selection (e.g., between the types of metal and the linker) allows to tailor their optical, electronic, and magnetic properties along with high porosity and surface area.

The luminescent MOFs have been proposed for several biological applications including molecular sensing, drug delivery, and imaging.[39−42] Despite many known advantages

Received: June 5, 2017
Accepted: September 11, 2017
Published: September 11, 2017

DOI: 10.1021/acsami.7b07818
ACS Appl. Mater. Interfaces 2017, 9, 33589−33598

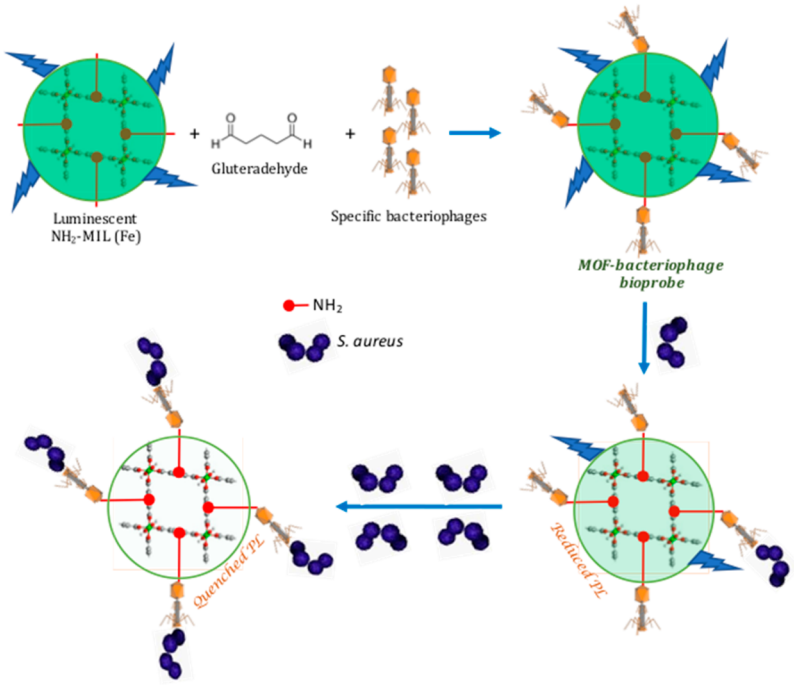

Figure 1. Schematic of NH_2-MIL53(Fe)−bacteriophage biosensor for PL-quenching-based detection of *S. aureus*.

(e.g., hierarchical structures and excellent optical properties under different environmental conditions), relatively little has been explored about the use of MOFs as fluorescent tags in bacterial assays. Indirect detection of bacteria has been proposed by analyzing their spores (e.g., dipicolinic acid (DPA)) using lanthanide-based MOFs such as $Eu_2(FMA)_2(OX)(H_2O)_4{\cdot}4H_2O$ and $Tb(BTC)(H_2O)_6$.[42,43] A specific interaction between lanthanide ion and DPA, followed by related changes in the photoluminescence (PL) intensity in the probe, could allow a selective detection of DPA. In case of $Eu_2(FMA)_2(OX)(H_2O)_4{\cdot}4H_2O$, the method involved a sensitive (about 0.5 ppm), selective, and instant "turn-on" sensing of bacterial endospores.[42] Tb-MOF ($Tb(BTC)(H_2O)_6$) is a water-dispersible compound with the potential for highly sensitive detection of DPA (limit of detection of 0.04 nM);[43] note that the presence of DPA caused the replacement of a Tb-BTC coordination mode with a Tb-DPA complex mode. This replacement influenced the energy transfer efficiency of the constituent metal ion (Tb^{3+}) so that a fluorescent quenching effect was endowed which was dependent on analyte concentration. In comparison to indirect approaches described above, a direct method was also recently proposed for the detection of *Staphylococcus arlettae* (*S. arlettae*) based on a fluorescent MOF, IRMOF-3.[35] However, such application was restricted by a relatively low aqueous stability of IRMOF-3 in context to sensor shelf life.

To design the biosensors for bacteria, the nanomaterials need to be conjugated with biomolecules (e.g., antibody, nucleic acids, and bacteriophages). The combinations of nanomaterials with antibodies and nucleic acids have been reported very frequently in the recent years.[44−47] Bacteriophages are the natural enemies of bacteria to represent an important class of biorecognition elements.[48,49] They are known to remain highly stable at a wide range of pH and temperature while allowing one to differentiate the live bacterium from the dead ones.[50] The wild-type bacteriophages have hence been employed for the detection of bacteria.[51−55] In most of these examples, the phage amplification assays that involve long incubation periods for the growth of bacteria were used preferably. In some of the studies, the bacteriophages have also been reported for direct electrochemical detection of bacteria.[56−58] In those examples, the tail proteins of the bacteriophages specifically interacted with the receptors present on bacterial cell surface. Recently, a bacteriophage conjugated IRMOF-3 has been reported for fluorescence-based detection of a nonpathogenic model bacterium *S. arlettae* with enhanced sensitivity.[35]

In the present work, we have developed an MOF−bacteriophage conjugate based biosensor for the detection of *Staphylococcus aureus* (*S. aureus*). A schematic of the working principle for the proposed biosensor is shown in Figure 1. The previously reported IRMOF-3/bacteriophage, when used as a bacterial probe, was seen to pose usability concerns because of a low aqueous stability.[35] To avoid such problems, we have explored in the present work, the use of a nontoxic, biocompatible, and water stable fluorescent MOF (i.e., NH_2-MIL-53(Fe)). The favorable properties of this MOF have been examined previously for a number of purposes including drug delivery, biomedical imaging, and sensing.[35,59,60]

The bacterium under study (i.e., *S. aureus*) is generally found on the skin and nostrils of about 25% of the healthy humans and animals.[61] However, certain toxins produced by *S. aureus* can lead to serious skin infections such as bacterimia and osteomyelitis.[62] *S. aureus* contamination in food has been linked with around 241 000 annual cases of food-borne illnesses in the United States alone.[2] As per the regulations of Food Development Authority (FDA), the tolerable limit of *S. aureus* in raw milk or other dairy products is recommended to be less than 10^4 CFU/g.[6,63] In some recent studies, concerns have been raised about exponential increase in the antibiotic resistance toward *S. aureus* strains, mainly methicillin-resistant *S. aureus* (MRSA).[64,65]

In view of the above facts, the development of rapid and sensitive detection methods for *S. aureus* has attained a paramount significance to ensure the regular monitoring and

DOI: 10.1021/acsami.7b07818
ACS Appl. Mater. Interfaces 2017, 9, 33589−33598

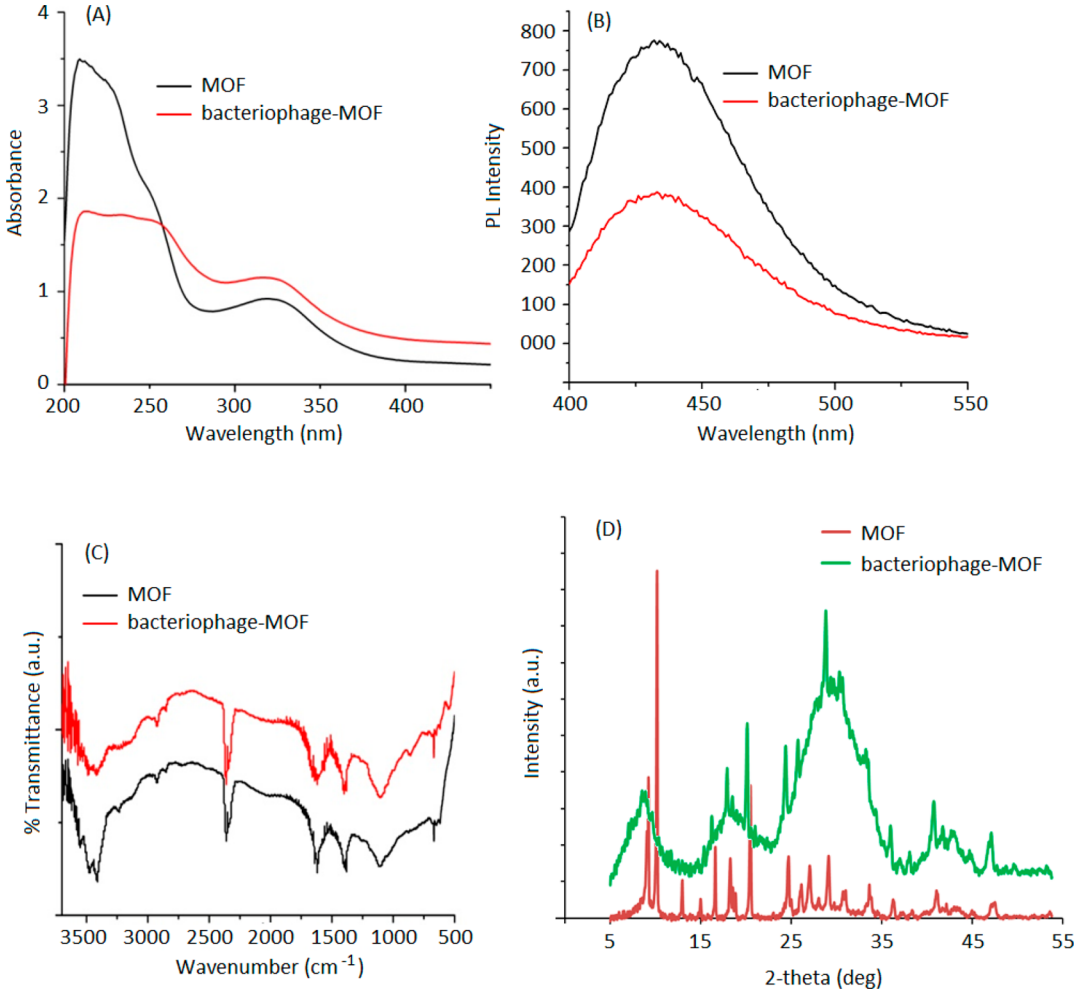

Figure 2. Characterization of NH_2-MIL-53 MOF before and after conjugation with bacteriophage: (A) UV−vis absorbance spectra; (B) PL spectra; (C) FTIR spectra; and (D) XRD pattern.

maintenance of the quality and hygiene of the different food products. In this paper, for the first time, we report a biosensor for *S. aureus* that is constituted of a water-dispersible fluorescent MOF (MIL-53-NH_2(Fe)) and a target-specific bacteriophage. Being structurally compatible with respect to their particle sizes (both the sensory material and biorecognition probe in micron sized particles), the integration of MOF and bacteriophages has allowed the construction of a highly sensitive and specific fluorescent sensing platform. This sensor system was stable for more than 100 days when stored under normal room temperature conditions, thereby showing the excellent usability for practical applications.

2. EXPERIMENTAL SECTION

2.1. Chemicals and Characterization Tools. Main reagents used in the study include $FeCl_3 \cdot 6H_2O$ (Ferric Chloride, Sigma), NH_2-BDC (2-aminobenzene-1,4-dicarboxylic acid; Sigma), gluteraldehyde (Sigma), Soya Casein Digest agar (SCD; Himedia), SCD broth (Himedia), and phosphate-buffered saline (PBS) buffer (Himedia). For the characterization of the samples, we employed a list of instrumentation including UV−vis spectrophotometer (UV−vis−NIR, Varian Cary 5000: scan rate (600 nm min^{-1}) and wavelength scanning range (200−450 nm)), Fourier-transform infrared spectroscope (FTIR, Nicolet, iS10; scan rate (2.5 cm/sec) and wavelength scanning range (500−4000 cm^{-1})), photoluminescence spectrophotometer (PL, Varian Cary; excitation wavelength (300 nm) and scan rate (600 nm/min)), field-emission scanning electron microscope (FESEM, Hitachi S4800; applied voltage (5−7 kV)), transmission electron microscopy (TEM, TECNAI G^2F-20), and X-ray diffractometer (XRD, Bruker, D8 Advance; 2θ range (0−55°), scan speed (4° min^{-1}), and step size (0.02)).

2.2. Synthesis of NH_2-MIL-53(Fe). The iron-based amine-functionalized NH_2-MIL-53 was prepared by solvothermal method.[66] Briefly, an equimolar mixture of $FeCl_3 \cdot 6H_2O$ (5 mmol) and NH_2-BDC (5 mmol) was prepared in deionized (DI) water. It was transferred to a sealed Teflon bottle and treated to autoclave heating at 150 °C for 3 days. The formed product (NH_2-MIL-53) was collected by filtration and washed twice with water and ethanol. Finally, the product was dried at 70 °C.

2.3. Conjugation of NH_2-MIL-53 with Target-Specific Bacteriophages. The bacteriophages specific to *S. aureus* were isolated and purified by following the procedure reported previously.[67] As the bacteriophages can proliferate where bacteria prevails, soil/waste samples were collected at some local bakery shops in Chandigarh, India. These samples were quickly brought into the laboratory and mixed with sterile water for centrifugation at 5000 rpm for 10 min. The supernatant containing bacteriophages was filtered through a 0.2 μm syringe filter for the separation from the remaining bacteria. The filtrate was then used for the isolation of bacteriophage by the double agar overlay procedure as described below. Briefly, 0.5 mL of sample filtrate was mixed with 0.3 mL of host bacterium grown overnight (i.e., *S. aureus*). A molten SCD top agar (0.6%) was then added to the above mixture. The resulting solution was immediately poured evenly onto the surface of sterile SCD agar plates. Clear plaques were formed on agar plates after incubation at 37 °C for 24 h. The individual plaques were picked from plates and then dissolved in

DOI: 10.1021/acsami.7b07818
ACS Appl. Mater. Interfaces 2017, 9, 33589−33598

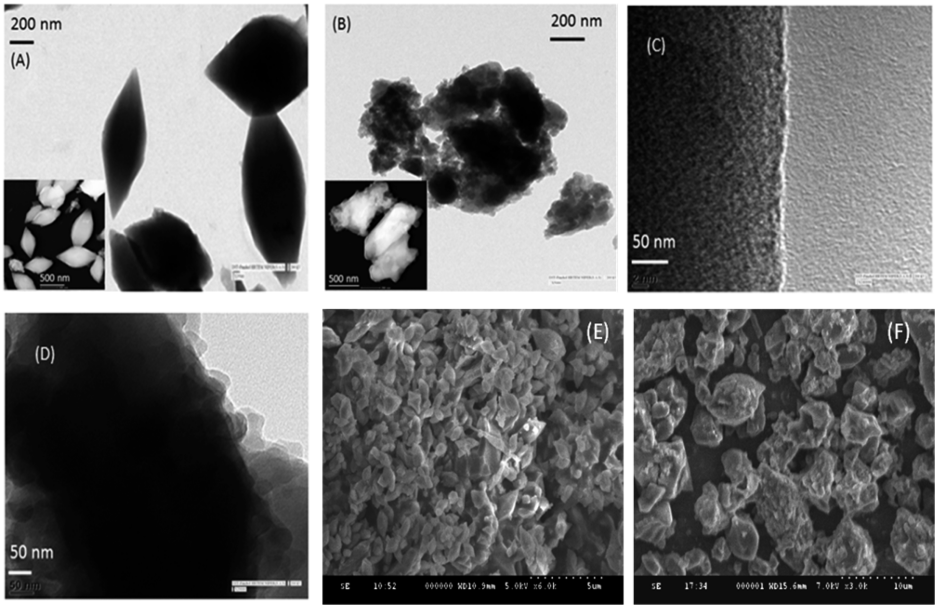

Figure 3. Structural images of the target MOF and their bacteriophage-loaded forms: (A) TEM image of NH_2-MIL-53 MOF, inset showing bright-field imaging of the sample; (B) TEM image of bacteriophage-loaded NH_2-MIL-53 MOF, inset showing bright-field imaging of the sample; (C) TEM of the edges of NH_2-MIL-53 MOF; (D) TEM of the edges of bacteriophage-loaded NH_2-MIL-53 MOF; (E) FE-SEM image of NH_2-MIL-53 MOF; and (F) FE-SEM image of bacteriophage-loaded NH_2-MIL-53 MOF.

PBS buffer. This solution was centrifuged at 6000 rpm for 10 min to allow the settling of bacterial and agar residues. The supernatant, containing isolated bacteriophages, was filtered through a sterilized filter membrane (0.22 μm). Furthermore, the titer of purified bacteriophages was amplified to 10^8 PFU/mL using an enrichment method.[68] Next, the enriched bacteriophage solution was mixed with NaCl and polyethylene glycol (PEG), followed by overnight incubation at 4 °C. The final concentrations of NaCl and PEG in solution were 10% (w/v) and 1 M, respectively. This step resulted in the precipitation of bacteriophages, which were then collected by centrifugation at 15 000 rpm (4 °C, 10 min). The precipitates were resuspended in 2−3 mL PBS and then treated with an equal volume of chloroform to remove PEG and bacterial cell debris.[69] A final bacteriophage titer of 10^8 PFU/mL was maintained by appropriate dilution with PBS buffer.

The isolated bacteriophages (specific to *S. aureus*) were covalently conjugated to the MOF surface using gluteraldehyde as a cross-linker. Briefly, 2 mg/mL MOF (NH_2-MIL-53) dispersion was prepared in 10 mL of PBS buffer (pH 7.4) and then mixed with 2 mL of the glutaraldehyde solution (25% in water). This mixture was incubated for 30 min at room temperature (RT, 25 ± 2 °C). The above glutaraldehyde-treated MOF (MOF-g) was subsequently separated from the solution by centrifugation.

For the preparation of MOF−bacteriophage complex, 15 mg of MOF-g was mixed with varying volumes (0.5−3 mL) of the stock bacteriophage solution. As the contents were left to react overnight, it caused the amine groups present on head of bacteriophage to bind with the MOF-g. The synthesized fluorescent molecular probe (MOF−bacteriophage) was separated from the reaction mixture by centrifugation. It was subsequently washed with PBS buffer and then stored at RT.

2.4. Test of MOF−Bacteriophage Complex's Activity toward *S. aureus*. The presence of active bacteriophages in the MOF−bacteriophage complex was determined by diffusion method. For this, the cultures of *S. aureus* grown overnight were spread over a solidified sterile SCD agar plate. A 100 μL sample of the NH_2-MIL-53 or MOF−bacteriophage was introduced in two different sections of the bacteria inoculated plate. The plate was then incubated overnight at 37 °C.

2.5. Detection of *S. aureus*. The MOF−bacteriophage complex has been employed for detection of *S. aureus* by measuring the changes in its photoluminescence (PL) intensity with respect to varying bacterial concentrations. A 400 μL sample of the MOF−bacteriophage solution (1 mg/mL) was incubated with 600 μL of 40−4 × 10^8 CFU/mL of *S. aureus* solution (in PBS) for 20 min (otherwise reported) at RT. After the reaction, the bacteria/MOF−bacteriophage complex was separated from the solution mixture by centrifugation at 5000 rpm. This step removed any unbound bacteria in the supernatant. The collected bacteria/bacteriophage-MOF sample was resuspended in 1 mL of PBS buffer. Control samples were run to compensate the dilution effects wherever required. The different bacteria/MOF−bacteriophage samples were then studied for their PL response at $\lambda_{excitation}$ of 300 nm. The specificity of the bacteriophage-MOF sensor toward *S. aureus* was evaluated against nonspecific *S. arlettae* and *Escherichia coli* bacteria. The developed method was also used for analysis of *S. aureus* in spiked samples of cream pastry. The same steps were adopted as those in the protocol described by Kotzekidou and co-workers.[70] Briefly, 20 g of a pastry sample was transferred aseptically into a sterile plastic bag. A solvent mixture of 0.1% w/v peptone, 0.085% w/v NaCl, and 0.1% v/v Tween 80 was then used to homogenize the sample. Further dilutions were made in sterile peptone water (0.1%). The experimental results obtained with the MOF−bacteriophage sensor were validated against those obtained by the standard colony counting method on similar samples.

3. RESULTS AND DISCUSSION

3.1. Absorption and Emission Characterization. In UV−vis absorption spectra (Figure 2A), the synthesized NH_2-MIL-53 has shown absorption peaks at 220, 250, and 340 nm due to −OH group sharing of FeO_6 octahedral clusters interconnected by the ligand (NH_2-BDC) molecules. The bacteriophage conjugation to the MOF was characterized by a protein-specific absorption peak at 279 nm which helped in confirming the desired formation of the MOF−bacteriophage sensor.

The PL spectra of the MOF and MOF−bacteriophage samples at an $\lambda_{excitation}$ of 300 nm are shown in Figure 2B. The MOF showed a characteristic emission peak at 430 nm. The photoluminescence of NH_2-MIL-53 is mainly attributed to amine substitution which acts as auxochromic as well as

DOI: 10.1021/acsami.7b07818
ACS Appl. Mater. Interfaces 2017, 9, 33589−33598

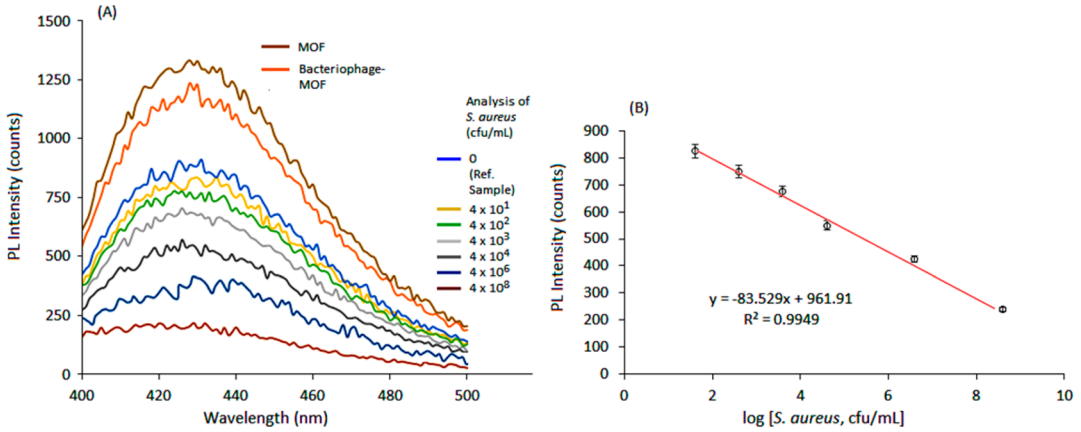

Figure 4. Calibration of MOF−bacteriophage complex system: (A) PL spectra of MOF−bacteriophage complex against different concentrations of *S. aureus* (40−4 × 10^8 CFU/mL) and (B) corresponding calibration curve.

bathochromic group to enhance charge transfer in the aromatic rings of synthesized MOF structure.[71] The unchanged PL signature of the MOF−bacteriophage sample indicated that this complex could be applied for the targeted application (e.g., fluorescent sensing of *S. aureus*). It was found that slight reduction took place in the emission intensity of the MOF−bacteriophage sample after the attachment of the protein. This can be related with the fact that in the case of MOF−bacteriophage complex both the involved moieties would compete for the absorption of the excitation energy light.

3.2. Structural and Morphological Characterizations of the Sensory Material. The FTIR studies have been carried out to investigate the formation of MOF and MOF−bacteriophage complex (Figure 2C). In case of the sample of NH_2-MIL-53 MOF, the peaks around 3100−3500 cm^{-1} signify the presence of amine groups, while those around 1600−1330 cm^{-1} reflect the symmetric and asymmetric vibrations of the carboxyl groups.[35,72] A peak around 1250−1270 cm^{-1} can be ascribed to the bidentate carbonate linker coordinated to the metal center. In the sample of MOF−bacteriophage, the appearance of an additional peak around 900 cm^{-1} suggests the δNH bending vibration of amines.[73] Thus, the FTIR studies confirmed a successful binding of the MOF with bacteriophages. The XRD of the NH_2-MIL-53 MOF (Figure 2D) matches the literature data.[66] The framework of NH_2-MIL-53 MOF is composed of −OH edge sharing FeO_6 octahedra interconnected by amino-BDC linkers to form one-dimensional pores as found in its parent molecule MIL-53(Fe).[74,75] The XRD pattern of the bacteriophage conjugated MOF retained most of the reference peaks. This investigation suggests that the MOF retained its structural integrity and crystalline nature despite the involvement of the aqueous processing steps undertaken to attach the bacteriophages over its surface.

The TEM (Figures 3A−D and S1) and FE-SEM imaging (Figure 3E,F) of the MOF and MOF−bacteriophage samples have also confirmed the presence of bacteriophage particles on the surface of the MOF. These images also verified the structural integrity of the MOF before and after the bioconjugation process. In TEM and SEM studies, it was confirmed that the crystallinity of the MOF was maintained even after its conjugation with the bacteriophages. The magnified structural images (TEM) of a MOF−bacteriophage sample, as presented in Figures 3A−D and S1, confirmed that the clear edges of the pure MOF sample took on an irregular shape after the attachment of the bioprobe. Figure S1 gives a fair indication about the oriented positioning (i.e., heads and tails lying perpendicular to the MOF surface) of the bacteriophages over the MOF surface. The final MOF−bacteriophage particles were almost homogeneous in their assembly.

The stability of the PL spectra on MOF−bacteriophage complex was examined across varying temperature conditions (20−50 °C). The data shown in Figure S2 indicated that MOF−bacteriophage complex could retain its PL properties over the investigated temperature range. This observation can be linked with the documented thermal stabilities of both MOF and bacteriophages. The activity of the MOF−bacteriophage complex was also confirmed by the spot test assay. A comparison of both MOF and MOF−bacteriophage against *S. aureus* is presented in Figure S3. The NH_2-MIL-53 alone did not exhibit any activity against the *S. aureus* bacteria although a clear zone appeared when it was conjugated with the bacteriophage particles. This result again clearly confirms the successful bioconjugation of the MOF with preserved bacteriophage activity.

3.3. Detection of *S. aureus*. To begin, the effect of the MOF−bacteriophage composition on the PL quenching was examined by controlling the proportion (w/v) of bacteriophages in the complex with respect to the best PL quenching results. To this end, 15 mg of MOF-g was mixed with varying quantities (0.5−3 mL) of the stock bacteriophage solution. After necessary preparatory steps (as mentioned in section 2.3), a dispersed sample of the prepared MOF−bacteriophage (400 μL of 1 mg/mL) probe was incubated with 600 μL of a fixed concentration (4 × 10^8 CFU/mL) of *S. aureus* for 20 min. The results of PL quenching for these MOF−bacteriophage solutions are plotted in Figure S4. The experiments revealed that the maximum PL quenching was attained when MOFs were mixed with bacteriophages in a weight/volume (w/v) ratio of 15 mg/2 mL. Consequently, in all other experiments, the fluorescent sensor was prepared by slightly adjusting that w/v ratio to 15 mg MOF/3 mL of bacteriophage (10^8 PFU/mL). Furthermore, the optimized response time for the MOF−bacteriophage sensor was studied by mixing and incubating the required volumes of the MOF−bacteriophage complex with a fixed concentration of the target bacteria for different time intervals. The results of this analysis are summarized in Figure S5. As the maximum PL quenching was attained for an incubation time of 15 min or more, all other sensing experiments were carried out over 20 min.

DOI: 10.1021/acsami.7b07818
ACS Appl. Mater. Interfaces 2017, 9, 33589−33598

Table 1. Comparison of Performance Parameters between Nanomaterials-Based Biosensors for *S. aureus*

order	nanomaterial	technique	limit of detection	detection range	reference
1	Fe_3O_4 NPs	MALDI-MS	7×10^4 CFU/mL		79
2	chitosan/CdS QDs	fluorescence	900 CFU/mL	10^3–10^7 CFU/mL	80
3	reduced graphene oxide	electrochemical impedance spectroscopy	100 fM		81
4	Co_3O_4-graphene nanocomposite	differential pulse voltammetry	4.3×10^{-13} M	1.0×10^{-12}–1.0×10^{-6} M	82
5	AuNPs	light scattering	10 CFU/mL		83
6	magnetic nanobeads/gold SAM	colorimetry	40 CFU/mL	75–7.5×10^6 CFU/mL	84
7	SWCNTs	potentiometry	800 CFU/mL	2.4×10^3–2.0×10^4 CFU/mL	85
8	NH_2-MIL-53	photoluminescence	31 CFU/mL	40–4×10^8 CFU/mL	This work

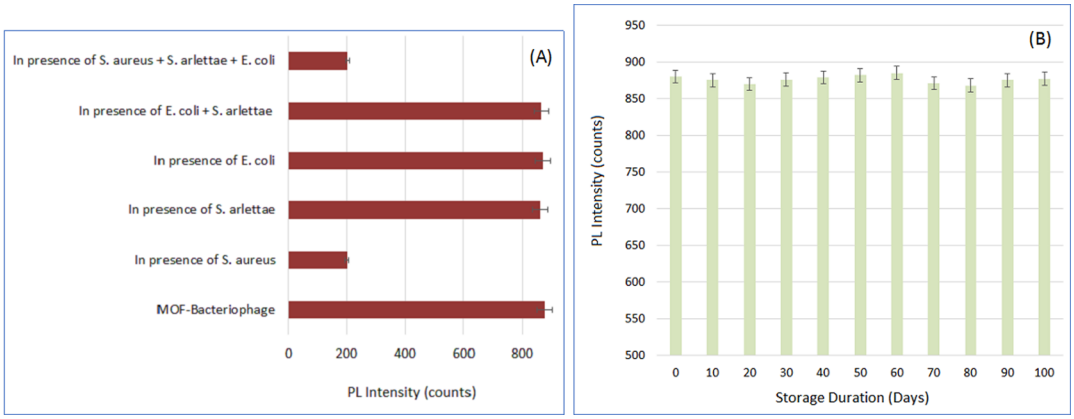

Figure 5. (A) Specificity of the proposed biosensor between the target bacteria *S. aureus* and potential interferences. Tests were made in the presence of target only and with others. The concentrations for bacteria in each sample was 4×10^8 CFU/mL. (B) Spectrophotometric characterization (PL studies) of the MOF–bacteriophage complex over storage duration of 0–100 days at room temperature.

The application of the bacteriophage-MOF as a fluorescent sensor for *S. aureus* (with respect to the varying concentrations between 40–4×10^8 CFU/mL) is demonstrated in Figure 4. The observed PL patterns (Figure 4A) and the corresponding calibration curve (Figure 4B) show decreasing fluorescence intensities in proportion to the bacterial concentrations tested. A linear pattern is attained within the concentration range of 40–4×10^8 CFU/mL. The observations clearly highlight the usefulness of the bacteriophage conjugated NH_2-MIL-53 as a highly sensitive sensory material for the optical detection of *S. aureus*. The decrease in the PL intensity of the bacteriophage–MOF complex upon its binding with the target bacteria can be attributed to the bacteriophage–bacteria interaction which causes a reduction in the effective excitation of the MOF due to competitive absorption of the light between different components involved in the system. The limit of detection (LOD) of the proposed sensor system for *S. aureus*, when assessed by the expression "3σ" (σ = standard deviation of measurements in the blank sample), was 31 CFU/mL. This LOD for *S. aureus* by the proposed sensor system is superior or comparable to those of many of the earlier fluorescent detection systems (Table 1).

3.4. Specificity, Stability, and Regeneration of the MOF–Bacteriophage Sensor. The specificity of the proposed biosensor was verified by testing it toward nonspecific bacteria (e.g., *S. arlettae* and *E. coli*). Figure 5A summarizes the original PL intensity of the sensory solution (i.e., MOF–bacteriophage) along with the observed changes in the PL intensity of MOF–bacteriophage complex toward *S. aureus*, *S. arlettae*, *E. coli*, mixture of *S. arlettae* + *E. coli*, and mixture of *S. aureus* + *E. coli* + *S. arlettae*. Clearly, the bacteriophage under study is highly specific toward the target *S. aureus* even in the individual or mixed presence of the nonspecific bacteria.

The long-term stability of the MOF–bacteriophage complex was investigated by intermittently recording its PL response toward *S. aureus* over a period of storage time. Note that this complex was stored at RT. Figure 5B depicts an insignificant change (i.e., lesser than 3%) in the PL response of the MOF–bacteriophage biosensor even after 100 days of storage. This observation has demonstrated the long-term stability of the proposed MOF–bacteriophage biosensor even under room-temperature storing conditions.

The crystalline integrity of the material was also tested by FE-SEM investigations. As depicted in Figure S6, the complex's crystalline nature was not degraded over the extended span of storage.

The regeneration of the MOF–bacteriophage complex was also attempted by washing the used material (5 min incubation with PBS buffer, followed by centrifugation step). The recycled material was then tested for the sensing of 4×10^8 CFU/mL *S. aureus* as per the steps described in section 3.3. The PL response of the MOF–bacteriophage during five such cycles is presented in Figure S7. The sensory material yielded satisfactory stable performance as there was only slight loss (e.g., about 10%) of the initial PL after five regeneration cycles. As demonstrated in this study, the regenerated bacteriophages were able to retain almost 90% of their initial activity. Note that other types of recognition moieties such as cell components (nucleic acid and antibodies) when regenerated may suffer from a significant loss of molecular activity; they became denatured or lost functionality to a degree in the presence of regeneration reagents like ethanolamine, glycine, phosphoric acid, and dilute HCl.[76,77] It should be ascribable to the fact that the

DOI: 10.1021/acsami.7b07818
ACS Appl. Mater. Interfaces 2017, 9, 33589–33598

Table 2. Analysis of Different (Diluted) Samples of Spiked Pastry Cream: Tests between MOF−Bacteriophage and Standard Colony Counting Method

	MOF−bacteriophage method			standard colony counting method	
sample no.	bacteria concentration (CFU/mL)	% recovery	relative standard deviation (in PL intensity)	bacteria concentration (CFU/mL)	% recovery
1	25 (±2) × 10^8	98−102	9.8	26 × 10^8	100
2	26 (±2) × 10^6	100−104	10.1	26 × 10^6	100
3	25 (±2) × 10^5	98−102	8.5	26 × 10^5	100
4	26 (±2) × 10^4	100−104	9.2	26 × 10^4	100
5	24 (±2) × 10^2	96−100	9.9	26 × 10^2	100

regeneration steps taken for our MOF−bacteriophage are much simpler than those practiced in other studies (e.g., the nanoparticle−antibody-based biosensor).[78]

3.5. Analysis of *S. aureus* in Spiked Cream Pastry Sample and Its Validation by Standard Method. The analysis of the spiked pastry cream samples (supernatant solution and its serial dilutions) with the MOF−bacteriophage biosensor is presented in Table 2. For the analysis, the observed PL intensity during the test was correlated with the standard calibration curve (Figure 4B). The analysis of the five serially diluted samples yielded the bacteria concentrations of 24 (±2) × 10^8, 26 (±2) × 10^6, 25 (±2) × 10^5, 26 (±2) × 10^4, and 24 (±2) × 10^2 CFU/mL. The above pastry cream samples were also analyzed with the standard colony counting method. The photographs of one of such representative analysis are shown in Figure S8. Comparison of the data, as shown in Table 2, highlights good agreement between the two contrasting approaches.

4. CONCLUSION

In this research, the performance of a convenient assembly of a MOF−bacteriophage-based biosensor was investigated for the sensitive and specific detection of *S. aureus* bacteria. Due to their structural compatibility (both the sensory material and recognition probe being micron sized particles), the proposed MOF−bacteriophage sensor probe was demonstrated to be successful in achieving the detection of the target bacteria in terms of enhanced reproducibility, stability, sensitivity, and specificity. The selected MOF (i.e., NH_2-MIL-53(Fe)) is a water-dispersible and stable structure. Its conjugation with the specific bacteriophages has offered the successful development of a new type of biosensor for *S. aureus*. The use of bacteriophages as the biorecognition probe has been realized to help in rendering a long-term stability as well as a regenerability of the biosensor. The performance of this sensing platform, when examined in terms of attained limit of detection of the method and the range of the linear analysis, is seen to be superior (or comparable) to those of many of the earlier biosensors employed for the detection of *S. aureus*.

In this study, the feasibility of NH_2-MIL-53(Fe) MOF−bacteriophage biosensor was explored against *S. aureus*. This sensing system is found to have high sensitivity, specificity, and regenerability while maintaining the excellent aqueous phase and temperature stability. In comparison to other nanomaterials tested previously for biosensing of bacteria (e.g., quantum dots, dye-doped nanoparticles, and carbon dots), the use of NH_2-MIL-53(Fe) offered a number of advantages. As a micrometer-sized fluorescent marker, NH_2-MIL-53(Fe) does not pose a concern of nanotoxicity as do QDs. This MOF can be patterned as a solid sensing substrate and is much easier to synthesize. Moreover, it also has a better structural compatibility with bacteriophages to retain stable PL emission across ranges of temperature. The assembly of hierarchical structures like MOF should also offer a precise control on particle size distribution (e.g., in terms of homogeneity) and purification from the precursors. As an iron based compound, NH_2-MIL-53(Fe) is nontoxic in nature, so it should be far safer to use as biosensors than the generally used quantum dots which contain harmful components like cadmium or lead.

■ ASSOCIATED CONTENT

Supporting Information

The Supporting Information is available free of charge on the ACS Publications website at DOI: 10.1021/acsami.7b07818.

TEM of MOF−bacteriophage complex, stability of PL emission of MOF−bacteriophage, spot test results to show activity of bare MOF and MOF−bacteriophage, optimization of MOF−bacteriophage composition, optimization of response time, FE-SEM of stored MOF−bacteriophage complex, results of regeneration of MOF−bacteriophage, data validation with colony counting method (PDF)

■ AUTHOR INFORMATION

Corresponding Authors

*E-mail: kkim61@hanyang.ac.kr. Tel.: +1-82-2-2220-2325. Fax: +82-2-2220-1945.

*E-mail: dr.akashdeep@csio.res.in. Tel: +91-172-2672236. Fax: +91-172-2657287.

ORCID

Ki-Hyun Kim: 0000-0003-0487-4242

Akash Deep: 0000-0002-6382-6104

Notes

The authors declare no competing financial interest.

■ ACKNOWLEDGMENTS

This work was funded through a CSIR India grant MLP 023. We are grateful to the Director of CSIR-CSIO, Chandigarh, India, for supporting this research. K.H.K. acknowledges support made in part by grants from the National Research Foundation of Korea (NRF) funded by the Ministry of Science, ICT & Future Planning (No. 2016R1E1A1A01940995). This work was also carried out with the support of "Cooperative Research Program for Agriculture Science and Technology Development (Project No. PJ012521032017)" Rural Development Administration, Republic of Korea.

■ REFERENCES

(1) Motarjemi, Y.; Käferstein, F.; Moy, G.; Quevedo, F. Contaminated Weaning Food: A Major Risk Factor for Diarrhoea and Associated Malnutrition. *Bull. W.H.O.* **1993**, *71* (1), 79.

(2) Kadariya, J.; Smith, T. C.; Thapaliya, D. Staphylococcus Aureus and Staphylococcal Food-Borne Disease: An Ongoing Challenge in Public Health. *BioMed Res. Int.* **2014**, *2014*, 1.
(3) Evans, M. R.; Ribeiro, C. D.; Salmon, R. L. Hazards of Healthy Living: Bottled Water and Salad Vegetables as Risk Factors for Campylobacter Infection. *Emerging Infect. Dis.* **2003**, *9* (10), 1219.
(4) Oliver, S. P.; Jayarao, B. M.; Almeida, R. A. Foodborne Pathogens in Milk and the Dairy Farm Environment: Food Safety And Public Health Implications. *Foodborne Pathog. Dis.* **2005**, *2* (2), 115−129.
(5) Aplin, J. *Presence of Coagulase-Negative Staphylococcus in Dairy Products*. Master of Science Thesis, Massey University, Palmerston North, New Zealand, 2014.
(6) Labbé, R. G.; García, S. *Guide to Foodborne Pathogens*; John Wiley & Sons: Chichester, U.K., 2013.
(7) Cho, I.-H.; Irudayaraj, J. In-Situ Immuno-Gold Nanoparticle Network ELISA Biosensors for Pathogen Detection. *Int. J. Food Microbiol.* **2013**, *164* (1), 70−75.
(8) Yu, H.; Zhao, G.; Dou, W. Simultaneous Detection of Pathogenic Bacteria using Agglutination Test based on Colored Silica Nanoparticles. *Curr. Pharm. Biotechnol.* **2015**, *16* (8), 716−723.
(9) Onori, M.; Coltella, L.; Mancinelli, L.; Argentieri, M.; Menichella, D.; Villani, A.; Grandin, A.; Valentini, D.; Raponi, M.; Russo, C. Evaluation of a Multiplex PCR Assay for Simultaneous Detection of Bacterial and Viral Enteropathogens in Stool Samples of Paediatric Patients. *Diagn. Microbiol. Infect. Dis.* **2014**, *79* (2), 149−154.
(10) Sheu, D.-S.; Wang, Y.-T.; Lee, C.-Y. Rapid Detection of Polyhydroxyalkanoate-Accumulating Bacteria Isolated from the Environment by Colony PCR. *Microbiology* **2000**, *146* (8), 2019−2025.
(11) Oblath, E. A.; Henley, W. H.; Alarie, J. P.; Ramsey, J. M. A Microfluidic Chip Integrating DNA Extraction and Real-Time PCR for the Detection of Bacteria in Saliva. *Lab Chip* **2013**, *13* (7), 1325−1332.
(12) Ivnitski, D.; Abdel-Hamid, I.; Atanasov, P.; Wilkins, E. Biosensors for Detection of Pathogenic Bacteria. *Biosens. Bioelectron.* **1999**, *14* (7), 599−624.
(13) Deisingh, A. K.; Thompson, M. Biosensors for the Detection of Bacteria. *Can. J. Microbiol.* **2004**, *50* (2), 69−77.
(14) Sanvicens, N.; Pastells, C.; Pascual, N.; Marco, M.-P. Nanoparticle-Based Biosensors for Detection of Pathogenic Bacteria. *TrAC, Trends Anal. Chem.* **2009**, *28* (11), 1243−1252.
(15) Ahmed, A.; Rushworth, J. V.; Hirst, N. A.; Millner, P. A. Biosensors for Whole-Cell Bacterial Detection. *Clin. Microbiol. Rev.* **2014**, *27* (3), 631−646.
(16) Razavi, H.; Janfaza, S. Medical Nanobiosensors: A Tutorial Review. *Nanomed. J.* **2015**, *2* (2), 74−87.
(17) Yoo, S. M.; Lee, S. Y. Optical Biosensors for the Detection of Pathogenic Microorganisms. *Trends Biotechnol.* **2016**, *34* (1), 7−25.
(18) Yan, J.; Estévez, M. C.; Smith, J. E.; Wang, K.; He, X.; Wang, L.; Tan, W. Dye-Doped Nanoparticles for Bioanalysis. *Nano Today* **2007**, *2* (3), 44−50.
(19) Wan, Y.; Sun, Y.; Qi, P.; Wang, P.; Zhang, D. Quaternized Magnetic Nanoparticles−Fluorescent Polymer System for Detection and Identification of Bacteria. *Biosens. Bioelectron.* **2014**, *55*, 289−293.
(20) Kim, G.; Moon, J.-H.; Moh, C.-Y.; Lim, J.-g. A Microfluidic Nano-Biosensor for the Detection of Pathogenic Salmonella. *Biosens. Bioelectron.* **2015**, *67*, 243−247.
(21) Duan, N.; Wu, S.; Dai, S.; Miao, T.; Chen, J.; Wang, Z. Simultaneous Detection of Pathogenic Bacteria Using an Aptamer Based Biosensor and Dual Fluorescence Resonance Energy Transfer from Quantum Dots to Carbon Nanoparticles. *Microchim. Acta* **2015**, *182* (5−6), 917−923.
(22) Frense, D.; Müller, A.; Beckmann, D. Detection of Environmental Pollutants using Optical Biosensor with Immobilized Algae Cells. *Sens. Actuators, B* **1998**, *51* (1), 256−260.
(23) Song, L.; Ahn, S.; Walt, D. R. Fiber-Optic Microsphere-Based Arrays for Multiplexed Biological Warfare Agent Detection. *Anal. Chem.* **2006**, *78* (4), 1023−1033.
(24) Kumar, J.; Jha, S. K.; D'Souza, S. Optical Microbial Biosensor for Detection of Methyl Parathion Pesticide using Flavobacterium Sp. Whole Cells Adsorbed on Glass Fiber Filters as Disposable Biocomponent. *Biosens. Bioelectron.* **2006**, *21* (11), 2100−2105.
(25) Michael, K. L.; Taylor, L. C.; Schultz, S. L.; Walt, D. R. Randomly Ordered Addressable High-Density Optical Sensor Arrays. *Anal. Chem.* **1998**, *70* (7), 1242−1248.
(26) Ko, S.; Grant, S. A. A Novel FRET-Based Optical Fiber Biosensor for Rapid Detection of Salmonella Typhimurium. *Biosens. Bioelectron.* **2006**, *21* (7), 1283−1290.
(27) Scheper, T.; Brandes, W.; Maschke, H.; Plötz, F.; Müller, C. Two FIA-Based Biosensor Systems Studied for Bioprocess Monitoring. *J. Biotechnol.* **1993**, *31* (3), 345−356.
(28) Doong, R.-A.; Tsai, H.-C. Immobilization and Characterization of Sol−Gel-Encapsulated Acetylcholinesterase Fiber-Optic Biosensor. *Anal. Chim. Acta* **2001**, *434* (2), 239−246.
(29) Ogert, R. A.; Brown, J. E.; Singh, B. R.; Shriver-Lake, L. C.; Ligler, F. S. Detection of Clostridium Botulinum Toxin A Using a Fiber Optic-Based Biosensor. *Anal. Biochem.* **1992**, *205* (2), 306−312.
(30) Yang, S.; Lin, X.; Blake, A. J.; Walker, G. S.; Hubberstey, P.; Champness, N. R.; Schröder, M. Cation-Induced Kinetic Trapping and Enhanced Hydrogen Adsorption in a Modulated Anionic Metal−Organic Framework. *Nat. Chem.* **2009**, *1* (6), 487−493.
(31) Murray, L. J.; Dincă, M.; Long, J. R. Hydrogen Storage in Metal−Organic Frameworks. *Chem. Soc. Rev.* **2009**, *38* (5), 1294−1314.
(32) Ma, L.; Falkowski, J. M.; Abney, C.; Lin, W. A Series of Isoreticular Chiral Metal−Organic Frameworks as a Tunable Platform For Asymmetric Catalysis. *Nat. Chem.* **2010**, *2* (10), 838−846.
(33) Takashima, Y.; Martínez, V. M.; Furukawa, S.; Kondo, M.; Shimomura, S.; Uehara, H.; Nakahama, M.; Sugimoto, K.; Kitagawa, S. Molecular Decoding using Luminescence from an Entangled Porous Framework. *Nat. Commun.* **2011**, *2*, 168.
(34) Kaur, R.; Sharma, A. L.; Kim, K.-H.; Deep, A. A Novel Cdte/Eu-MOF Photoanode for Application in Quantum Dot-Sensitized Solar Cell to Improve Power Conversion Efficiency. *J. Ind. Eng. Chem.* **2017**, *53*, 77−81.
(35) Bhardwaj, N.; Bhardwaj, S. K.; Mehta, J.; Nayak, M. K.; Deep, A. Bacteriophage Conjugated IRMOF-3 as a Novel Opto-Sensor For S. Arlettae. *New J. Chem.* **2016**, *40* (9), 8068−8073.
(36) Vellingiri, K.; Kumar, P.; Deep, A.; Kim, K.-H. Metal-Organic Frameworks for the Adsorption of Gaseous Toluene under Ambient Temperature and Pressure. *Chem. Eng. J.* **2017**, *307*, 1116−1126.
(37) Mehta, J.; Bhardwaj, N.; Bhardwaj, S. K.; Kim, K.-H.; Deep, A. Recent Advances in Enzyme Immobilization Techniques: Metal-Organic Frameworks as Novel Substrates. *Coord. Chem. Rev.* **2016**, *322*, 30−40.
(38) Song, F.; Wang, C.; Falkowski, J. M.; Ma, L.; Lin, W. Isoreticular Chiral Metal− Organic Frameworks for Asymmetric Alkene Epoxidation: Tuning Catalytic Activity by Controlling Framework Catenation and Varying Open Channel Sizes. *J. Am. Chem. Soc.* **2010**, *132* (43), 15390−15398.
(39) Zhao, X.; Fang, J.; Li, Y.; Huang, C. Highly Selective Recognition of Adenosine 5′-Triphosphate Against other Nucleosides Triphosphate with a Luminescent Metal-Organic Framework of [Zn (BDC)(H2O)2] n (BDC= 1, 4-benzenedicarboxylate). *Sci. China: Chem.* **2013**, *56* (11), 1651−1657.
(40) Zhang, S.-Y.; Shi, W.; Cheng, P.; Zaworotko, M. J. A Mixed-Crystal Lanthanide Zeolite-like Metal−Organic Framework as a Fluorescent Indicator for Lysophosphatidic Acid, A Cancer Biomarker. *J. Am. Chem. Soc.* **2015**, *137* (38), 12203−12206.
(41) Rieter, W. J.; Taylor, K. M.; Lin, W. Surface Modification and Functionalization of Nanoscale Metal-Organic Frameworks for Controlled Release and Luminescence Sensing. *J. Am. Chem. Soc.* **2007**, *129* (32), 9852.
(42) Xu, H.; Rao, X.; Gao, J.; Yu, J.; Wang, Z.; Dou, Z.; Cui, Y.; Yang, Y.; Chen, B.; Qian, G. A Luminescent Nanoscale Metal−Organic Framework with Controllable Morphologies for Spore Detection. *Chem. Commun.* **2012**, *48* (59), 7377−7379.

DOI: 10.1021/acsami.7b07818
ACS Appl. Mater. Interfaces 2017, 9, 33589−33598

(43) Bhardwaj, N.; Bhardwaj, S.; Mehta, J.; Kim, K.-H.; Deep, A. Highly Sensitive Detection of Dipicolinic Acid with a Water-Dispersible Terbium-Metal Organic Framework. *Biosens. Bioelectron.* **2016**, *86*, 799−804.
(44) Mehta, J.; Bhardwaj, N.; Bhardwaj, S. K.; Tuteja, S. K.; Vinayak, P.; Paul, A.; Kim, K.-H.; Deep, A. Graphene Quantum Dot Modified Screen Printed Immunosensor for the Determination of Parathion. *Anal. Biochem.* **2017**, *523*, 1−9.
(45) Bhardwaj, S. K.; Sharma, A. L.; Bhardwaj, N.; Kukkar, M.; Gill, A. A.; Kim, K.-H.; Deep, A. TCNQ-Doped Cu-Metal Organic Framework as a Novel Conductometric Immunosensing Platform for the Quantification Of Prostate Cancer Antigen. *Sens. Actuators, B* **2017**, *240*, 10−17.
(46) Liu, X.; Wang, F.; Aizen, R.; Yehezkeli, O.; Willner, I. Graphene Oxide/Nucleic-Acid-Stabilized Silver Nanoclusters: Functional Hybrid Materials for Optical Aptamer Sensing and Multiplexed Analysis of Pathogenic Dnas. *J. Am. Chem. Soc.* **2013**, *135* (32), 11832−11839.
(47) Wu, H.; Shi, H.; Zhang, H.; Wang, X.; Yang, Y.; Yu, C.; Hao, C.; Du, J.; Hu, H.; Yang, S. Prostate Stem Cell Antigen Antibody-Conjugated Multiwalled Carbon Nanotubes for Targeted Ultrasound Imaging and Drug Delivery. *Biomaterials* **2014**, *35* (20), 5369−5380.
(48) Singh, A.; Poshtiban, S.; Evoy, S. Recent Advances in Bacteriophage Based Biosensors for Food-Borne Pathogen Detection. *Sensors* **2013**, *13* (2), 1763−1786.
(49) Brovko, L. Y.; Anany, H.; Griffiths, M. W. 6 Bacteriophages for Detection and Control of Bacterial Pathogens in Food and Food-Processing Environment. *Adv. Food Nutr. Res.* **2012**, *67*, 241.
(50) Schmelcher, M.; Loessner, M. J. Application of Bacteriophages for Detection of Foodborne Pathogens. *Bacteriophage* **2014**, *4* (2), e28137.
(51) Shabani, A.; Zourob, M.; Allain, B.; Lawrence, M.; Mandeville, R. Electrochemical Detection of Bacteria using Bacteriophage. *ISSSE* **2007**, 45−47.
(52) Singh, A.; Glass, N.; Tolba, M.; Brovko, L.; Griffiths, M.; Evoy, S. Immobilization of Bacteriophages on Gold Surfaces for the Specific Capture of Pathogens. *Biosens. Bioelectron.* **2009**, *24* (12), 3645−3651.
(53) Hagens, S.; Loessner, M. J. Application of Bacteriophages for Detection and Control of Foodborne Pathogens. *Appl. Microbiol. Biotechnol.* **2007**, *76* (3), 513−519.
(54) Klumpp, J.; Loessner, M. J. Detection of Bacteria with Bioluminescent Reporter Bacteriophage. *Adv. Biochem. Eng./Biotechnol.* **2014**, *144*, 155−171.
(55) Anany, H.; Chou, Y.; Cucic, S.; Derda, R.; Evoy, S.; Griffiths, M. From Bits and Pieces to Whole Phage to Nanomachines: Pathogen Detection using Bacteriophages. *Annu. Rev. Food Sci. Technol.* **2017**, *8*, 305−329.
(56) Bhardwaj, N.; Bhardwaj, S. K.; Mehta, J.; Mohanta, G. C.; Deep, A. Bacteriophage Immobilized Graphene Electrodes for Impedimetric Sensing of Bacteria (Staphylococcus Arlettae). *Anal. Biochem.* **2016**, *505*, 18−25.
(57) Shabani, A.; Zourob, M.; Allain, B.; Marquette, C. A.; Lawrence, M. F.; Mandeville, R. Bacteriophage-Modified Microarrays for the Direct Impedimetric Detection of Bacteria. *Anal. Chem.* **2008**, *80* (24), 9475−9482.
(58) Yemini, M.; Levi, Y.; Yagil, E.; Rishpon, J. Specific Electrochemical Phage Sensing for Bacillus Cereus and Mycobacterium Smegmatis. *Bioelectrochemistry* **2007**, *70* (1), 180−184.
(59) Horcajada, P.; Chalati, T.; Serre, C.; Gillet, B.; Sebrie, C.; Baati, T.; Eubank, J. F.; Heurtaux, D.; Clayette, P.; Kreuz, C.; et al. Porous Metal-Organic-Framework Nanoscale Carriers as a Potential Platform for Drug Delivery and Imaging. *Nat. Mater.* **2010**, *9* (2), 172−178.
(60) Chowdhuri, A. R.; Bhattacharya, D.; Sahu, S. K. Magnetic Nanoscale Metal Organic Frameworks for Potential Targeted Anticancer Drug Delivery, Imaging and as An MRI Contrast Agent. *Dalton Trans.* **2016**, *45* (7), 2963−2973.
(61) Centers for Disease Control and Prevention. Staphylococcal Food Poisoning. https://www.cdc.gov/foodsafety/diseases/staphylococcal.html (accessed on September 10, 2017).
(62) Centers for Disease Control and Prevention. *Staphylococcus aureus* in Healthcare Settings. https://www.cdc.gov/hai/organisms/staph.html (accessed on September 10, 2017).
(63) U.S. Department of Health and Human Services Food and Drug Administration Guidance for FDA Staff: Compliance Policy Guide Sec. 527.300 Dairy Products - Microbial Contaminants and Alkaline Phosphatase Activity (CPG 7106.08) (Draft). December 2009, https://www.fda.gov/downloads/ICECI/ComplianceManuals/CompliancePolicyGuidanceManual/UCM192468.pdf (accessed on September 10, 2017).
(64) Laxminarayan, R.; Duse, A.; Wattal, C.; Zaidi, A. K.; Wertheim, H. F.; Sumpradit, N.; Vlieghe, E.; Hara, G. L.; Gould, I. M.; Goossens, H. Antibiotic Resistance—The Need for Global Solutions. *Lancet Infectious Diseases* **2013**, *13* (12), 1057−1098.
(65) Ventola, C. L. The Antibiotic Resistance Crisis: Part 1: Causes and Threats. *Pharm. Ther.* **2015**, *40* (4), 277−283.
(66) Wang, D.; Huang, R.; Liu, W.; Sun, D.; Li, Z. Fe-Based Mofs for Photocatalytic CO2 Reduction: Role of Coordination Unsaturated Sites and Dual Excitation Pathways. *ACS Catal.* **2014**, *4* (12), 4254−4260.
(67) Bhardwaj, N.; Bhardwaj, S.; Devi, P.; Dahiya, S.; Singla, M.; Ghanshyam, C.; Minakshi, P. Phage Immobilized Antibacterial Silica Nanoplatform: Application against Bacterial Infections. *Adv. Anim. Vet. Sci.* **2015**, *3* (1s), 1−9.
(68) Kropinski, A. M.; Mazzocco, A.; Waddell, T. E.; Lingohr, E.; Johnson, R. P. Enumeration of Bacteriophages by Double Agar Overlay Plaque Assay. *Methods Mol. Biol.* **2009**, *501*, 69−76.
(69) Yamamoto, K. R.; Alberts, B. M.; Benzinger, R.; Lawhorne, L.; Treiber, G. Rapid Bacteriophage Sedimentation in the Presence of Polyethylene Glycol and its Application to Large-Scale Virus Purification. *Virology* **1970**, *40* (3), 734−744.
(70) Kotzekidou, P. Microbiological Examination of Ready-To-Eat Foods and Ready-to-Bake Frozen Pastries from University Canteens. *Food Microbiol.* **2013**, *34* (2), 337−343.
(71) Wen, L.; Zhou, L.; Zhang, B.; Meng, X.; Qu, H.; Li, D. Multifunctional Amino-Decorated Metal−Organic Frameworks: Nonlinear-Optic, Ferroelectric, Fluorescence Sensing and Photocatalytic Properties. *J. Mater. Chem.* **2012**, *22* (42), 22603−22609.
(72) Ellison, M. D.; Gasda, P. J. Functionalization of Single-Walled Carbon Nanotubes with 1, 4-Benzenediamine using a Diazonium Reaction. *J. Phys. Chem. C* **2008**, *112* (3), 738−740.
(73) Mehta, J.; Vinayak, P.; Tuteja, S. K.; Chhabra, V. A.; Bhardwaj, N.; Paul, A.; Kim, K.-H.; Deep, A. Graphene Modified Screen Printed Immunosensor for Highly Sensitive Detection of Parathion. *Biosens. Bioelectron.* **2016**, *83*, 339−346.
(74) Llewellyn, P.; Horcajada, P.; Maurin, G.; Devic, T.; Rosenbach, N.; Bourrelly, S.; Serre, C.; Vincent, D.; Loera-Serna, S.; Filinchuk, Y.; et al. Complex Adsorption of Short Linear Alkanes in the Flexible Metal-Organic-Framework MIL-53 (Fe). *J. Am. Chem. Soc.* **2009**, *131* (36), 13002−13008.
(75) Haque, E.; Khan, N. A.; Park, J. H.; Jhung, S. H. Synthesis of a Metal−Organic Framework Material, Iron Terephthalate, by Ultrasound, Microwave, and Conventional Electric Heating: A Kinetic Study. *Chem. - Eur. J.* **2010**, *16* (3), 1046−1052.
(76) Dill, K. A.; Shortle, D. Denatured States of Proteins. *Annu. Rev. Biochem.* **1991**, *60* (1), 795−825.
(77) Lang, E. Physical-Chemical Limits for the Stability of Biomolecules. *Adv. Space Res.* **1986**, *6* (12), 251−255.
(78) Huang, J.; Yang, G.; Meng, W.; Wu, L.; Zhu, A.; Jiao, X. An Electrochemical Impedimetric Immunosensor for Label-Free Detection of Campylobacter Jejuni in Diarrhea Patients' Stool Based on O-Carboxymethylchitosan Surface Modified Fe3O4 Nanoparticles. *Biosens. Bioelectron.* **2010**, *25* (5), 1204−1211.
(79) Lin, Y.-S.; Tsai, P.-J.; Weng, M.-F.; Chen, Y.-C. Affinity Capture using Vancomycin-Bound Magnetic Nanoparticles for the MALDI-MS Analysis of Bacteria. *Anal. Chem.* **2005**, *77* (6), 1753−1760.
(80) Wang, X.; Du, Y.; Li, Y.; Li, D.; Sun, R. Fluorescent Identification and Detection of Staphylococcus Aureus with

DOI: 10.1021/acsami.7b07818
ACS Appl. Mater. Interfaces 2017, 9, 33589−33598

Carboxymethyl Chitosan/Cds Quantum Dots Bioconjugates. *J. Biomater. Sci., Polym. Ed.* **2011**, *22* (14), 1881−1893.
(81) Wang, Z.; Zhang, J.; Chen, P.; Zhou, X.; Yang, Y.; Wu, S.; Niu, L.; Han, Y.; Wang, L.; Chen, P.; et al. Label-Free, Electrochemical Detection of Methicillin-Resistant Staphylococcus Aureus DNA with Reduced Graphene Oxide-Modified Electrodes. *Biosens. Bioelectron.* **2011**, *26* (9), 3881−3886.
(82) Qi, X.; Gao, H.; Zhang, Y.; Wang, X.; Chen, Y.; Sun, W. Electrochemical DNA Biosensor with Chitosan-Co 3 O 4 Nanorod-Graphene Composite for the Sensitive Detection of Staphylococcus Aureus Nuc Gene Sequence. *Bioelectrochemistry* **2012**, *88*, 42−47.
(83) Chang, Y.-C.; Yang, C.-Y.; Sun, R.-L.; Cheng, Y.-F.; Kao, W.-C.; Yang, P.-C. Rapid Single Cell Detection of Staphylococcus Aureus by Aptamer-Conjugated Gold Nanoparticles. *Sci. Rep.* **2013**, *3*, 1863.
(84) Suaifan, G. A.; Alhogail, S.; Zourob, M. Rapid and Low-Cost Biosensor for the Detection of Staphylococcus Aureus. *Biosens. Bioelectron.* **2017**, *90*, 230−237.
(85) Zelada-Guillén, G. A.; Sebastián-Avila, J. L.; Blondeau, P.; Riu, J.; Rius, F. X. Label-Free Detection of Staphylococcus Aureus in Skin using Real-Time Potentiometric Biosensors Based on Carbon Nanotubes and Aptamers. *Biosens. Bioelectron.* **2012**, *31* (1), 226−232.

DOI: 10.1021/acsami.7b07818
ACS Appl. Mater. Interfaces 2017, 9, 33589−33598